Complementary Methods for Human Visual Perception of Visual Weather Lore Sky Objects Using Machine Learning Methods

Mwanjele Mwagha
Department of Informatics and Computing
Taita Taveta University
Voi, Kenya
soproltd@gmail.com

Muthoni Masinde
Department of Information Tehnology
Central University of Technology
Bloemfontein, South Africa
muthonimasinde@gmail.com

***Abstract*—Recent research indicate a surge in the use of machine learning and artificial intelligence to compliment the processes of human visual perception. In particular, applying closeness measures of digital objects is of great significance in the attempts to account for the correspondence between digitized sky objects and some human identifiable object. The scoring of computerized objects can be based on testing a combination of well-known features humans use for visual perception, with a consideration that the human visual cognition system is well tailored for discriminating structural information from visual objects. This way, benchmark tests can be used to compute some proximity of detected objects to the specified object's reality. Apart from producing outputs for use in the predictions, object similarity tests can also act as a mechanism for quality assessment process for the results of computer object detectors. One assumption here is that similar objects cannot qualify as perfect matches to their real objects but may contain some acceptable divergence in their closeness. In this paper, algorithms for extracting shape, color and texture information in visual sky (specific to traditional weather lore) objects are investigated as candidates for visual sky objects benchmarking, and their performances compared using a collection of positive/negative instances of visual sky objects. The rationale for testing both positive/negative instances was due to the fact that while the sky objects detectors can be expected to generate positive detections, the number of false positives detectable should be negligible.**

Keywords—image_representation;; image_similarity; weather lore; bag_of_words; hog; visual perception; image detection; image recognition

I. INTRODUCTION

The computer vision image analysis approach is quite different from human vision. It is challenging for the computer to perform image perception in real dimensional space and employ background knowledge as in the case with human beings [1]. The recognition and extraction of features that fully reveal the content of images is current research in computer vision [2, 4] for it is critical to find dependable correspondence between sets of images [5].

Image feature recognition and retrieval has been highly studied [6,7]. A number of algorithms have been tested [8] but still not found to be perfect when working with shadowed and low-contrasted images [9]. Clutter in image background horizon [13, 10], increases dimensionality which passes a challenge in the process of feature extraction when there are fewer training samples [15]. Image recognition in varying appearance and illumination is also problematic [16, 17]. The mentioned challenges bring visual ambiguity [19] leading to ineffective representations in image categorization [20] which lead to producing approximate classification results. In some image-processing tasks, low-level visual image features retrieved may not correspond to high-level image semantics [21].

There are many image data complexity issues [22], prompting computer vision researchers to propose de-noising before image processing [23]. Research suggests a need to make image colors be constant to ensure that the supposed color of images stands out with changes in lighting [24]. Other research reveals that working with only one classifier cannot deal efficiently with the complete task of image classification [25]. There is also a need to select suitable feature spaces for use in the construction of image classification models [26].

Visual or observed weather lore is mostly used by indigenous societies to come up with weather predictions. In order to realize the integration of visual weather lore in modern weather forecasting systems, there is need to represent and scientifically verify this form of knowledge. The remaining part of the paper is structured as follows: section two reviews the various procedures involved in image processing. Section three describes the methods involved in the processing of images. In section four the results are discussed while

978-1-7281-3464-2/19/$31.00 ©2019 IEEE

section five and six is on conclusions and future work respectively.

II. RELATED LITERATURE

A. Representation of Image Features

Image features extraction (the process of locating specific points in an image) is an essential step before image recognition [4,27-29]. In video applications, feature extraction is used to estimate the trajectory of an object in the image plane [2]. Current research in image recognition and retrieval has been focused on extracting different visual features of an object in order to identify the object from the image [30-32] with the intention of allowing computer applications and users to search or recognize specific objects in an image [30,31,33,34]. Image features are also known as the signatures of the image [28,35].

The task of image feature extraction can only be complete when objects have been identified and recognized by the machine [33]. The purpose of image feature extraction is to represent an image in compact and unique form of single values or matrix vectors [23,30,36]. In this process, the visual content of the images is mapped into a new feature vector [35,37,38]. To improve performance and memory management after image extraction, only appropriate features are selected to reduce the number of features used in the image classification task [19,38,39].

B. Extraction of Image Features

The human eye perceives images with a combination of features including: -color, texture, and shape [40]. The key to a working computer vision system is the choice of features extracted to represent an image [35,41]. Visual object distinguishable features that can be extracted include:- color, texture and shape [29,31-33,38,42,43]. Once these visual image features have been extracted, the image retrieval and recognition process reduces to measuring the similarities between the features [31]. Other basic features that can be used to recognize visual objects include contour, diameter, length, width, area, perimeter, size, shape, composition and location [44-47].

C. Techniques of Extracting Image Features

The techniques of geometry-based feature extraction (Gabor wavelet transform), appearance based techniques, color segmentation based techniques, template based feature color histograms, color moments and edge histogram descriptors are used to extract image features [48,49]. The choice of a technique relies on factors such as image scale, illumination variation, variation noise and orientation [32,48]. The feature extraction techniques chosen must enhance the discriminative power of feature descriptors making the classification task less difficult [50,51]. An extraction technique that is able to retain the neighborhood associations among image pixels is advantageous [35]. Programming tools are available for image feature extraction with diversity of methods to describe the properties of visual objects [27].

D. Machine Learning for Industrial Revolution

Research has shown that there is some complementarity between machine learning technologies and the skill level of human experts [68]. Artificial intelligence and machine learning have become a trend in society development [69]. With the growing reliance on technology [70], the fourth industrial revolution has stimulated the advancement of science and technology [66]. There has been increased application of artificial intelligence, high-tech algorithms, mobile sensors, 3-D printing, and unmanned vehicles in transforming all aspects of human society including strategic governance [67], lifestyle, industry and employment [71, 72].

III. METHODOLOGY

A. Data Source

A collection of sky objects for experimentation were captured using a sky camera installed at CUT BHP building with GPS location and from secondary sources (repository of NASA images and in www.flikr.com). Image comparison methods were subjected to bulk data sets containing 1000 images per sky object and in varying situations such as scale and illumination.

B. Object Similarity Checks

The process of checking similarity (`Figure 1`) between extracted and ideal objects involves computing the distance or the difference between the objects. Similar objects will have a distance of zero, while the distance between objects increases as the objects increasingly becomes more different. This process is vital to supplement the object detection procedure in the eventuality of false positives. The image color, shape and texture intensity variations (specified as benchmarks or similarity scores) are the output in this process.

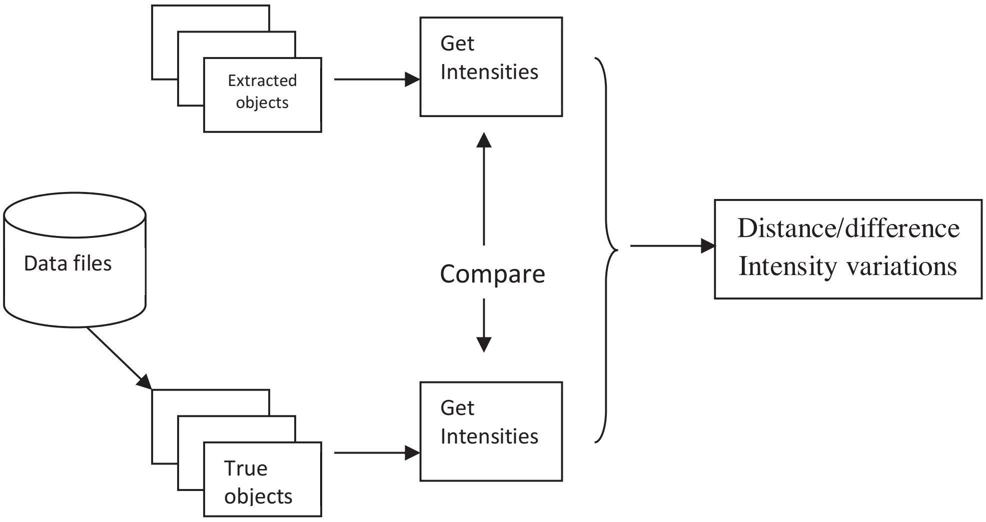

Figure 1: Similarity Check between Detected and True Objects

C. Shape-based Benchmark Tests

Shape is an important low level feature that can be used to recognize images for indexing and retrieval [13,43,52-55]. Human eye exploit shapes to identify and recognize the real world objects [4]. In shape based image retrieval, the similarity between shapes represented by their features is measured [38,56].

The Histogram of oriented gradients (HOG) features of extracted sky object were generated by first computing the magnitudes of gradients and their orientations (directions) over the entire object. The magnitude of the gradients was computed using equation 1 below:

$$|G| = \sqrt{I_x^2 + I_y^2} \quad\text{............................}(1)$$

And the orientation of the gradients was computed using equation 2 below:

$$\theta = \arctan\frac{I_y}{I_x} \quad\text{...............................}(2)$$

The gradients that had small magnitudes were transformed to zeros. The image grid cells were aligned to the object position. Orientation histograms were generated for each object cell, by quantizing the gradient directions. The gradient thresholds were added in orientation bins. The orientation histograms were stacked into one vector of length N*C. (The value of N represented the number of orientation bins while the values C representing the number of object cells.) After stacking the resultant vector was normalized to a unit length with the normalization factor using either of the equations 3 to 5:

$$f = \sqrt{\frac{v}{\|v\|_1 + e}} \quad\text{..........................}(3)$$

$$f = \frac{v}{\|v\|_1 + e} \quad\text{...........................}(4)$$

$$f = \frac{v}{\|v\|_2^2 + e^2} \quad\text{.........................}(5)$$

The unit vector consisted of the HOG features that uniquely represented the extracted sky object.

D. Edge Based Benchmark Tests

Edge detection methods were used to discover points in extracted sky objects where brightness changed abruptly (mathematically referred to as discontinuity). The discontinued points in extracted objects were organized into sets of segments with curved lines (edges). Edge features were extracted objects using the canny and Laplacian of Gaussian (LoG) edge detection algorithms.

The Canny edge algorithm aims at the derivation of an optimal smoothing filter for minimizing multiple responses to single edge detections. In Canny, the edge points are determined using points in an image where the magnitude of gradients presume local maximum in the gradient direction.

The procedure of deriving a Canny edge in extracted sky objects follows these steps:

(a) The first step was to apply a Gaussian smoothing filter to an extracted sky object using equation 6 below:

$$S[i,j] = G[i,j,\sigma] * I[i,j] \text{.............}(6)$$

The value I [i,j] represented the extracted object; G[i,j,σ] was the Gaussian smoothing filter, and σ was the spread of the Gaussian that was used to control the smoothing degree. The outcome of the convolution of an extracted object with the Gaussian filters led to an array matrix representing a smoothed object S[i, j].

(b) The second step was to calculate the magnitudes of gradients and orientations in the smoothed objects. This was achieved by using gradient of the smoothed array matrix S[i, j] to generate x and y partial derivatives, followed by applying the finite-difference method to approximate the partial derivatives. See equation 7 below:

$$\left.\begin{aligned} \frac{\partial S}{\partial x} &= S[i,j] * Gx \\ \frac{\partial S}{\partial y} &= S[i,j] * Gy \\ M[i,j] &= \sqrt{\frac{\partial S}{\partial x}^2 + \frac{\partial S}{\partial y}^2} \\ \theta[i,j] &= \arctan\left(\frac{\partial S / \partial y}{\partial S / \partial x}\right) \end{aligned}\right\} \text{.......}(7)$$

(c) The third step was to establish object edge directions by applying non-maxima suppression to the magnitudes of the gradients. Successful establishment of the edge directions was followed by the alignment of the edges to the directions that can be traced in an object. For each and every pixel (i,j) in an object some the direction was computed that can best approximate the direction of the object pixel.

(d) The final step was applying the double threshold algorithm that links edges in an object.

The Laplacian of Gaussian edge feature extraction process was done in two steps. The first step was to apply a Laplacian derivative filter to determine areas of abrupt variation (or edges) in an extracted object. The second step was to smooth the object by applying the Gaussian filter in equation 9.

$$L(x,y) = \nabla^2 f(x,y) = \frac{\partial^2 f(x,y)}{\partial x^2} + \frac{\partial^2 f(x,y)}{\partial y^2} \text{....}(9)$$

The Laplacian and Gaussian functions can be combined to obtain a single equation that includes the smoothing Gaussian filter in equation 10:

$$LoG(x,y) = -\frac{1}{\pi\sigma^4}\left[1 - \frac{x^2 - y^2}{2\sigma^2}\right] e^{-\frac{x^2+y^2}{2\sigma^2}} \text{......}(10)$$

The LoG (Laplacian of Gaussian) operator obtained the second derivative of the object. Object parts that are uniform gave LoG values of zero, while abrupt changes occurring in an object gave LoG values that were positive.

E. Texture -Based Benchmark Tests

Texture is a very important feature in the analysis and classification of images [22,42,57,58]. Texture relates to visual patterns with properties of homogeneity and can be said to be fine, uniform, dense, coarse, or smooth; rippled, irregular, or lineated [41,59]. In texture visual patterns can also be described in terms of granularity, directionality, and repetitiveness [60]. An image texture is a metric that can be used to depict in sequence the spatial arrangement of color or intensities in an image. Texture is an important feature in distinguishing image contents. Various methods (such as Entropy and GLCM) were used to extract texture in sky objects.

Entropy measured the randomness to represent the texture of an extracted sky object using the equation 11 below:

sum (p.*log2 (p)). …………(11)

The value p was a count of object histograms that were determined from an RGB object. Mathematically the entropy can be represented by equation 12:

$$Ent_i = \frac{1}{MN}\sum_{x=1}^{M}\sum_{y=1}^{N} I_i(x,y)(-\ln I_i(x,y)) \text{.....}(12)$$

where $I_i(x,y)$ is an object with dimension MxN.

The procedures of calculating extracted objects texture features utilized the values of the GLCM to measure the variation in intensity or texture between extracted object pixels. A GLCM comprises information regarding the locations of object pixels that have similar grey levels. To come up with a GLCM a displacement vector $d=(dx,dy)$ was determined. From the vector d, pairs of image pixels that have grey levels (i,j) and separation d were counted. A nxn dimensional GLCM was formed, where n is the number of grey levels determined from an extracted sky object.

F. *Color Based Benchmark Tests*

Color is an important and widely used feature for visual object representation [41,61-63]. Human vision system uses color for recognition and discrimination of objects (Bhardwaj, Di, R. Hamid, Piramuthu, & Sundaresan, 2013; Nikolaou & Papamarkos, 2002; Tian, 2013; Jun Zhang, Barhomi, & Serre, 2012).
Color was not reliable in detection tasks, since visual objects changed color subject to geometric transformations and varying illumination. However, in the task of matching predefined sky objects, color information proved important. To compare extracted sky objects the three independent color channels (red, green and blue) were extracted from the pairs of detected objects and designated real objects for matching purpose.
The Euclidean Distance (Delta-E) is a single number representing the distance between color channels images. Delta-E was determined by calculating the Euclidean distance difference between the red, green and blue channels in extracted objects and designated real objects. The change in the distance ΔE_{ab} between the objects was computed by using equation 13

$$\Delta E^{*}_{xy} = \sqrt{\left(r^{*}_{x}-r^{*}_{y}\right)^{2}+\left(g^{*}_{x}-g^{*}_{y}\right)^{2}+\left(b^{*}_{x}-b^{*}_{y}\right)^{2}} \quad ....(13)$$

where $r*$ is the red color channel, $g*$ is the green color channel and $b*$ the blue color channel of the objects (x= designated real object; y=extracted object).
The technique of (SSIM) index was used in determining the correspondence between extracted object and designated real objects. The SSIM measure was considered as a quality comparison of an image to another image that is of perfect quality. In SSIM the designated real object was assumed to be a perfect and distortion-free image. The SSIM index was measured on a range of common-size windows of extracted object and designated real object. Given two windows (x=designated real object and y=extracted object), of size N×N the SSIM was determined by:

$$SSIM(x,y)=\frac{(2\mu_x\mu_y+c_1)(2\sigma_{xy}+c_2)}{(\mu_x^2+\mu_y^2+c_1)(\sigma_x^2+\sigma_y^2+c_2)} \quad ....(15)$$

IV. RESULTS AND DISCUSSION

A. *Benchmarks of Visual Objects*

A specification of benchmark sky objects was provided for each sky object. The benchmark formed the designated real object for evaluating the quality (similarity) of detected target sky objects. In appropriate circumstance two benchmark sky objects were specified for the day and night images respectively. The dimensions of the benchmarks were transformed to common size of 252 by 127 pixels. The day and night images (Table 1) were designated dynamically based on the time meta-data of detected sky scene.

Table 1: Designated Real Sky objects

Sky Object	Day Image	Night Image
high clouds		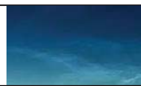
low clouds		
medium clouds		
clear sky	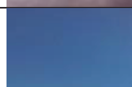	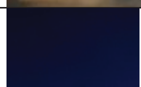
stars		
rainbow	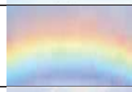	
lightning		
dark moon		
visible moon		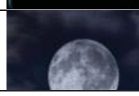

B. *Comparison between the Benchmarks*

The above bench mark tests were subjected to bulk data sets containing 1000 images per sky concept and in three varying sets of situations. Detected sky objects were subjected for similarity benchmark; the preferred scores were greater than or equal to 0.5 for detected sky objects. A transformation function was used in parallel with benchmarks tests to account for the percentage of objects benchmarked with scores greater than 0.5 in each of the three situations. The rationale for setting scores greater than 0.5 was that the extracted sky objects were expected to resemble an average similarity to their corresponding designated real objects. The comparison algorithm is as follows: -

```
read (bulk image set)
n=number of objects;
for object=1:n
    begin
    count=0;
    detection procedure;
        if(detected)
        extract
        procedure;
        benchmark
        procedure;
            if(bench
            mark>th
            reshold)
            count=c
            ount+1;
            else
            count=c
            ount;
            endif
        else
        count=count;
        endif
    performance=count/n*100
    ;
end for
```

The benchmark results (Table 2) were useful in comparing the similarity check methods. The percentage scores for each feature were represented in the table, with the best measure identified in the last column.

Table 1: Performance of Measures for Benchmarking Instances to Designated real objects

Visual Sky Objects	Percent of Scores>0.5 per 1000 Samples of Positive Instances							
	Delta E (Color Based)	SSIM (Color Based)	Canny (edge Based)	log (edge Based)	Entropy (Texture)	GLCM (Texture Based)	HOG (Shape Based)	Selected Method
High clouds	88.3333	26.6667	41.6667	41.6667	88.3333	88.3333	88.3333	HOG
Low clouds	96.7742	16.1290	58.0645	54.8387	100	100	100	HOG
Medium clouds	100	19.3548	67.7419	67.7419	100	100	100	HOG
Clear sky	80.4878	78.0488	4.8780	4.8780	80.4878	80.4878	80.4878	HOG
Stars	40.4762	2.3810	23.8095	35.7143	100	88.0952	100	HOG
Rainbow	68.7500	0	0	0	75	75	75	HOG
Lightning	84.4444	0	93.3333	95.5556	93.3333	88.8889	100	HOG
Dark moon	32	32	100	96	100	100	100	HOG
Visible moon	80.4020	48.7437	0	0	83.4171	83.4171	83.4171	HOG

V. CONCLUSIONS

It is worth to note that shape based features (HOG) descriptors performed best in both detection and benchmarking of sky concepts. This was evident by the higher overall detection and benchmark rates compared to other features.

The procedure of benchmarking-extracted sky objects used appropriate day or night objects to score the detected sky objects. Confidence levels on the final sky concepts were determined based on complementary and supplementary relationships between the benchmarked sky objects. The three measures (detections, benchmarks, and confidence) in determining sky concepts were meant to increase model self-reliance in representing sky concepts. The final sky concepts were structured and represented in the form of a mathematical vector, for use in the predictions component.

The results on weather image processing for similarity checking and resemblance creates a basis upon which traditional visual weather lore can be scientifically verified and incorporated in modern weather prediction systems.

VI. FURTHER WORK

Combined benchmarking of features can be realized by linking set of features (such as color; texture; shape; and edge) that are unique to sky objects. The major importance of combining features to benchmark sky objects is that there are rare possibilities for effects of shared features to be ambiguous. An assumption is that two or more sky objects with the same color features could not have the identical edge, shape and texture features. While the computation of collective feature histograms is computationally more intensive (since tests and comparisons for several features needed to be processed) than tests for single a feature it can lead to better performance when matching sky objects.

VII. REFERENCES

[1] Yang, “Information Mining From Remote Sensing Imagery Based On Multi-Scale And Multi-Feature Processing Techniques,” The International Archives of the Photogrammetry, Remote Sensing and Spatial Information Sciences, vol. 38, 2009, pp. 158-161.

[2] P. Kamavisdar, S. Saluja, and S. Agrawal, “A Survey on Image Classification Approaches and Techniques,” International Journal of Advanced Research in Computer and Communication Engineering, vol. 2, 2013, pp. 1005-1009.

[3] L. R and A.A. S, “Facial Feature Extraction in Color Images Based on Local Binary Pattern,” International Journal of Science and Research, vol. 3, 2014, pp. 545-547.

[4] D.P. Tian, “A Review on Image Feature Extraction and Representation Techniques,” International Journal of Multimedia and Ubiquitous Engineering, vol. 8, 2013, pp. 385-396.

[5] M.P. Babu and P.R. Shankar, “A Novel Algorithm for Color Image matching using Wavelet-SIFT,” International Journal of Scientific and Research Publications, vol. 5, 2015, pp. 1-6.

[6] G. Lavoué, “Bag of Words and Local Spectral Descriptor for 3D Partial Shape Retrieval,” EurographicsWorkshop on 3D Object Retrieval, 2011.

[7] S. Sukhpreet, “Optical Character Recognition Techniques : A survey,” International Journal of Advanced Research in Computer Engineering & Technology, vol. 2, 2013, pp. 2009-2015.

[8] N.S. Wadhe, S.W. Mohod, and N.N. Khalsa, “An Overview – Artificial Neural Network Based Advanced Face and Non-Face Recognition,” International Journal of Engineering Studies and Technical Approach, vol. 01, 2015, pp. 1-10.

[9] C. Nagaraju, B. Srinu, and E.S. Rao, “An efficient Facial Features extraction Technique for Face Recognition system Using Local Binary Patterns,” International Journal of Innovative Technology and Exploring Engineering, vol. 2, 2013, pp. 76-78.

[10] T. Khatib, H. Karajeh, H. Mohammad, and L. Rajab, “Full Length Research Paper A hybrid multilevel text extraction algorithm in scene images,” academicJournals, vol. 10, 2015, pp. 105-113.

[11] K. Subba and R. Naga, “Feature Extraction for Image Classification and Analysis with Ant Colony Optimization Using Fuzzy Logic Approach,” Signal & Image Processing : An International Journal, vol. 2, 2011, pp. 137-143.

[12] K. Etemad and R. Chellappa, “Discriminant analysis for recognition of human face images,” Journal of Optical Society of America, vol. 14, 1997, pp. 1724-1733.

[13] J. Calbo and J. Sabburg, “Feature Extraction from Whole-Sky Ground-Based Images for Cloud-Type Recognition,” American Meteorological Society, 2008, pp. 3-14.

[14] Y.G. Jiang, Y. Jun, and N. Chongwah, “Towards Optimal Bag-of-Features for Object Categorization and Semantic Video Retrieval,” Association of Computing Machinery, 2007.

[15] J. Xudong, M. Bappaditya, and K. Alex, “Complete discriminant evaluation and feature extraction in kernel space for face recognition,” Machine Vision and Applications, vol. 20, 2009, pp. 35-46.

[16] K.-wai Wong, K.-man Lam, and W.-chi Siu, “An effcient algorithm for human face detection and facial feature extraction under different conditions,” Pattern Recognition Society. Published by Elsevier Science Ltd., vol. 34, 2004, pp. 1993-2004.

[17] J.K. Appati, G.O. Fosu, and G.K. Gogovi, “Face Feature Extraction for Recognition Using Radon Transform,” American Journal of Engineering Research, vol. 3, 2014, pp. 219-224.

[18] W. John, Y. Allen, G. Arvind, and S. Shankar, “Robust Face Recognition via Sparse Representation,” IEEE Transactions On Pattern Analysis And Machine Intelligence, vol. 31, 2009, pp. 1-18.

[19] K. Rahat, B. Cécile, M. Damien, and C. Ducottet, “Spatial histograms of soft pairwise similar patches to improve the bag-of-visual-words model,” Computer Vision and Image Understanding, vol. 132, 2015, pp. 102-112.

[20] E. Nowak, F. Jurie, and B. Triggs, “Sampling Strategies for Bag-of-Features,” Springer-Verlag Berlin Heidelberg, 2006, pp. 490-503.

[21] Y. Deng, B.S. Manjunath, C. Kenney, M.S. Moore, and H. Shin, "An Efficient Color Representation for Image Retrieval," IEEE Transactions On Image Processing, vol. 10, 2001, pp. 140-147.
[22] M. Benco, R. Hudec, P. Kamencay, M. Zachariasova, and S. Matuska, "An Advanced Approach to Extraction of Color Texture Features Based on GLCM," International Journal of Advanced Robotic Systems ARTICLE, vol. 11, 2014, pp. 1-8.
[23] S. Soma and B.V. Dhandra, "Automatic Logo Recognition System from The Complex Document Using Shape and Moment Invariant Features," International Journal of Advances in Computer Science and Technology, vol. 4, 2015, pp. 06 - 13.
[24] Z. Jun and B. Youssef, "Color Image Descriptor," Springer-Verlag Berlin Heidelberg, 2012, pp. 312-324.
[25] D.F. Lorca, M.Á. Sotelo, L.M. Bergasa, P.R.D. Toro, J. Nuevo, M. Ocaña, M. Ángel, and G. Garrido, "Combination of Feature Extraction Methods for SVM Pedestrian Detection," IEEE Transactions On Intelligent Transportation Systems, vol. 8, 2007, pp. 292-307.
[26] Y. Yuan, M. Minjing, and Z. Menglu, "Cloud Detection Method Based On Feature Extraction In Remote Sensing Images Abstract :," International Archives of the Photogrammetry, Remote Sensing and Spatial Information Sciences, vol. XL-2/W1, 2013, pp. 173-177.
[27] L.A. Ruiz, J.A. Recio, A. Fernández-Sarría, and T. Hermosilla, "A Tool For Object Descriptive Feature Extraction : Application To Image Classification And Map Updating," The International Archives of the Photogrammetry, Remote Sensing and Spatial Information Sciences, vol. XXXVIII-4/, 2009.
[28] N. Jain and S.S. Salankar, "Color & Texture Feature Extraction for Content Based Image Retrieval," IOSR Journal of Electrical and Electronics Engineering, vol. 2014, 2014, pp. 53-58.
[29] S. Vijayarani and S. Priyatharsini, "Comparative Analysis of Facial Image Feature Extraction Algorithms," Journal of Multidisciplinary Engineering Science and Technology, vol. 2, 2015, pp. 107-112.
[30] S. Kuril and I. Saini, "Cloud Classification for Weather Information by Artificial Neural Network," International Journal of Applied Physics and Mathematics, vol. 3, 2013, pp. 28-30.
[31] A. Thakur and A. Dhole, "Object Recognition From Image Using Grid Based Color Moments Feature Extraction Method," International Journal of Research in Engineering and Technology, 2013, pp. 333-336.
[32] A. Olaode, G. Naghdy, and C. Todd, "Unsupervised Classification of Images : A Review," International Journal of Image Processing, vol. 5, 2014, pp. 325-342.
[33] R. Saritha and C. Parthasarathy, "An Efficient Information - driven Framework for Image Mining," International Journal of Current research and Academic Review, vol. 2, 2014, pp. 171-178.
[34] K.K. Pachouri, "A Comparative Analysis & Survey of various Feature Extraction Techniques," International Journal of Computer Science and Information Technologies, vol. 6, 2015, pp. 377-379.
[35] N. Nikolaou and N. Papamarkos, "Color image retrieval using a fractal signature extraction technique," Engineering Applications of Artificial Intelligence, vol. 15, 2002, pp. 81-96.
[36] M.V.K.P.T. Ponuchamy, "Feature Extraction and Classification of Blood Cells Using Artificial Neural Network," American Journal of Applied Sciences, vol. 9, 2012, pp. 615-619.
[37] S.N. Kakarwal and R.R. Deshmukh, "Hybrid Feature Extraction Technique for Face Recognition," International Journal of Advanced Computer Science and Applications, vol. 3, 2012, pp. 60-64.
[38] R.S. Chora, "Image Feature Extraction Techniques and Their Applications for CBIR and Biometrics Systems," International Journal Of Biology And Biomedical Engineering, Vol. 1, 2007, Pp. 6-16.
[39] Pradeep, "D Iagonal Based F Eature E Xtraction For Handwritten A Lphabets R Ecognition," International Journal of Computer Science & Information Technology, vol. 3, 2011, pp. 27-38.
[40] M. Benčo and R. Hudec, "Novel Method for Color Textures Features Extraction Based on GLCM," Radio Engineering, vol. 16, 2007, pp. 64-67.
[41] G. Sridhar, "Color and Texture Based Image Retrieval," ARPN Journal of Systems and Software, vol. 2, 2012, pp. 1-6.
[42] K. Wasim, K. Shiv, G. Neetesh, and K. Nilofar, "A Proposed Method for Image Retrieval using Histogram values and Texture Descriptor Analysis," International Journal of Soft Computing and Engineering, vol. 1, 2011, pp. 33-36.
[43] P. Mohanaiah, P. Sathyanarayana, and L. Gurukumar, "Image Texture Feature Extraction Using GLCM Approach," International Journal of Scientific and Research Publications, vol. 3, 2013, pp. 1-5.
[44] J. Piera, V. Baradad, E. García-LadonaParisi-, A. Lombarte, L. Recasens, and J. Cabestany, "Otolith shape feature extraction oriented to automatic classification with open distributed data," Marine And Freshwater Research, 2005, pp. 805-814.
[45] R.V.R. Chary, D.R. Lakshmi, and K.V.N. Sunitha, "F Eature E Xtraction M Ethods For Color Image Similarity," Advanced Computing: An International Journal, vol. 3, 2012, pp. 147-157.
[46] Sindhu, "A Survey on Detecting Brain Tumorinmri," International Journal of Innovative Research in Computer and Communication Engineering, vol. 3, 2015, pp. 123-129.
[47] M. Faizal, A. Jabal, S. Hamid, S. Shuib, and I. Ahmad, "Leaf Features Extraction And Recognition Approaches To Classify Plant," Journal of Computer Science, vol. 9, 2013, pp. 1295-1304.
[48] S. Dhawan and H. Dogra, "Feature Extraction Techniques for Face Recognition," International Journal of Engineering, Business and Enterprise Applications, vol. 12, 2012, pp. 1-4.
[49] R.S. Dubey, R. Choubey, and J. Bhattacharjee, "Multi Feature Content Based Image Retrieval," International Journal on Computer Science and Engineering, vol. 02, 2010, pp. 2145-2149.
[50] S. Yang, "Discriminative Data Transform for Image Feature Extraction and Classification," Springer-Verlag Berlin Heidelberg, 2013, pp. 452-459.
[51] G. Vamvakas, B. Gatos, and S.J. Perantonis, "A Novel Feature Extraction and Classification Methodology for the Recognition of Historical Documents," 10th International Conference on Document Analysis and Recognition, IEEE, 2009, pp. 491-495.
[52] S. Mathew and V. Balas, Zachariah, "A Content-based Image Retrieval System Based On Convex Hull Geometry," Acta Polytechnica Hungarica, vol. 12, 2015, pp. 103-116.
[53] B. Ramesh, C. Xiang, and T.H. Lee, "Shape classification using invariant features and contextual information in the bag-of-words model," Pattern Recognition Society. Published by Elsevier Science Ltd., vol. 48, 2015, pp. 894-906.
[54] L. Xiaolan, G. Afzal, and W. Asim, "Spatially Enhanced Bags of Words for 3D Shape Retrieval," Springer-Verlag Berlin Heidelberg, 2008, pp. 349-358.

[55] R. Toldo, U. Castellani, and A. Fusiello, "A Bag of Words Approach for 3D Object Categorization," Springer-Verlag Berlin Heidelberg, 2009, pp. 116-127.
[56] Hermosilla, "Combining Features Extracted From Imagery And Lidar Data For Object-Oriented Classification Of Forest Areas," The International Archives of the Photogrammetry, Remote Sensing and Spatial Information Sciences, vol. XXXVIII-4/, 2005, pp. 3-8.
[57] R. Ramana, R. Mani, and V. Kumar, "Classification of Textures Based on Features Extracted from Preprocessing Images on Random Windows," International Journal of Advanced Science and Technology, vol. 9, 2009, pp. 9-18.
[58] S. Al-momen, L.E. George, and R.K. Naji, "Texture classification using spline , wavelet decomposition and fractal dimension," Applied and Computational Mathematics, vol. 4, 2015, pp. 5-10.
[59] R.M. Haralick and K. Shanmugam, "Textural Features for Image Classification," IEEE Transactions On Systems, Man, And Cybernetics, vol. SMC-3, 1973.
[60] N. Mishra and S. Silakari, "Image Mining in the Context of Content Based Image Retrieval :," International Journal of Computer Science Issues, vol. 9, 2012, pp. 69-76.
[61] G. Mandloi, "A Survey on Feature Extraction Techniques for Color Images," Journal of Computer Science, vol. 5, 2014, pp. 4615-4620.
[62] Y. Zhao and X. Zhai, with Rongrong, "Recaptured Images Forensics Based On Color Moments and DCT Coefficients Features," Journal of Information Hiding and Multimedia Signal Processing, vol. 6, 2015, pp. 323-333.
[63] F. Alamdar and M. Keyvanpour, "A New Color Feature Extraction Method Based on Dynamic Color Distribution Entropy of Neighborhoods," International Journal of Computer Science Issues, vol. 8, 2011, pp. 42-48.
[64] B. Anurag, H. Raffay, P. Robinson, and S. Neel, "Palette Power : Enabling Visual Search through Colors," KDD-Association of Computing Machinery, Chicago, Illinois: Association of Computing Machinery, 2013.
[65] J.R. Smith and S.-fu Chang, "Single Color Extraction and Image Query," International Conference on Image Processing, 1995, pp. 1-4.
[66] Y. Liao, E. Rocha, F. Deschamps, and G. Brezinski, "The impact of the fourth industrial revolution : a cross-country / region comparison," Production, vol. 5411, 2018.
[67] S. S. Vempati, "India And The Artificial Intelligence Revolution," Carnegie Endow. Int. Peace, 2016.
[68] D. M. West, "employment and public policy," no. October, 2015.
[69] B. Diffey and A. Korikov, "The application and development of artificial intelligence in smart clothing The application and development of artificial intelligence in smart clothing," in IOP Conf. Series: Materials Science and Engineering, 2018.
[70] M. Masayuki, "The Effects of Artificial Intelligence and Robotics on Business and Employment : Evidence from a survey on Japanese firms," Res. Inst. Econ. Trade Ind., vol. 16-E-066, 2016.
[71] A. Thierer, A. C. O. Sullivan, and R. Russell, "Artificial Intelligence and Public Policy," Mercat. Cent. Georg. Mason Univ., 2017.
[72] S. Makridakis, "The Forthcoming Artificial Intelligence (AI) Revolution : Its Impact on Society and Firms," Neap. Univ. PAPHOS, no. 01, 2017.